Body-Wave Methods of Distinguishing between Explosions, Collapses, and Earthquakes: Application to Recent Events in North Korea

by William R. Walter, Douglas A. Dodge, Gene Ichinose, Stephen C. Myers, Michael E. Pasyanos, and Sean R. Ford

ABSTRACT

Examination of regional distance seismic data from historic nuclear test sites has led to a variety of very effective discriminants between explosions, earthquakes, and collapses. We focus on the body-wave methods. We show that ratios between *P*- and *S*-wave amplitudes (*P*/*S* ratios) above about ~2 Hz very effectively separate the six Democratic People's Republic of Korea (DPRK) declared nuclear tests between 2006 and 2017 from natural earthquakes in the region. Similarly, *P*/*S* ratios separate historic Nevada Test Site (NTS) nuclear explosions from western U.S. earthquakes. We show that combining *P*/*S* ratios with ratios of low-frequency to high-frequency *S*-wave amplitudes can effectively separate postexplosion collapse events, such as the 1982 NTS Atrisco collapse, and the apparent collapse that followed about eight and a half minutes after the 3 September 2017 DPRK explosion. Explosions often produce fewer and smaller aftershocks than comparably sized earthquakes, which has been proposed as a potential discriminant. We apply the body-wave techniques to the recent seismicity following the largest DPRK event, after first using correlation methods to build a more complete catalog of these events. Despite the empirical effectiveness of the regional body-wave discriminants, the physical basis for the generation of explosion *S* waves, and therefore the predictability of *P*/*S* and low/high frequency techniques, as a function of path, frequency, and event properties such as size, depth, and geology, remains incompletely understood. A goal of current research, such as the Source Physics Experiments (SPE), is to improve our physical understanding of the mechanisms of explosion *S*-wave generation and advance our ability to numerically model and predict them.

INTRODUCTION

The recent magnitude 6.1 (International Data Center [IDC][1] m_b) declared underground nuclear test by the Democratic People's Republic of Korea (DPRK) is the largest in more than 20 years, following the cessation of nuclear testing by signatories of the Comprehensive Nuclear-Test-Ban Treaty (CTBT) in 1996. Since that time only nonsignatory countries have declared nuclear tests, and only DPRK has declared tests in this century. The 3 September 2017 declared nuclear test was the sixth since DPRK began testing in 2006. It was by an order of magnitude, the largest nuclear test in the DPRK series (the next largest on 9 September 2016 had an IDC m_b of 5.1) and has been followed by additional seismicity, including an apparent cavity collapse and nearby seismic events reported by the U.S. Geological Survey (USGS) and others. In this paper we apply regional distance body-wave methods to both the recent DPRK events, as well as historic events in Nevada, to better understand the DPRK area seismicity and evaluate their discrimination effectiveness.

There has been a large amount of work over many years to find methods to reliably separate and identify explosions from a background of natural earthquakes (e.g., National Research Council [NRC] report, 2012). Among the most robust methods of discriminating earthquakes from explosions are ratios of regional *P*/*S* amplitudes at high frequencies (e.g., Walter *et al.*, 1995; Taylor, 1996; Hartse *et al.*, 1997; Kim *et al.*, 1997; Battone *et al.*, 2002; Rodgers and Walter, 2002; Taylor *et al.*, 2002). These techniques make use of regional *P* and *S* waves traveling in the crust (*Pg* and *Lg*) and regional *P* and *S* waves traveling in the uppermost mantle (*Pn* and *Sn*). These regional techniques allow event identification to be extended to much lower magnitudes than older empirical teleseismic techniques, such as $M_s : m_b$ (e.g., Bowers and Selby, 2009; Selby *et al.*, 2012).

There is relatively less work on methods to separate seismic events associated with the collapse of underground cavities from explosions and earthquake. Nevertheless, some effective methods are known (e.g., Taylor, 1994; Pechmann *et al.*, 1995; Mine Seismicity Report and the Comprehensive Nuclear-Test-Ban Treaty, 1999; Bowers and Walter, 2002). Recent work using regional waveform modeling-based moment tensor values show clear separation between the three types of events (Ford *et al.*, 2009). However, such methods rely on intermediate

[1]The International Data Center (IDC) is a component of the Preparatory Commission for the Comprehensive Nuclear Test Ban Treaty Organization.

doi: 10.1785/0220180128

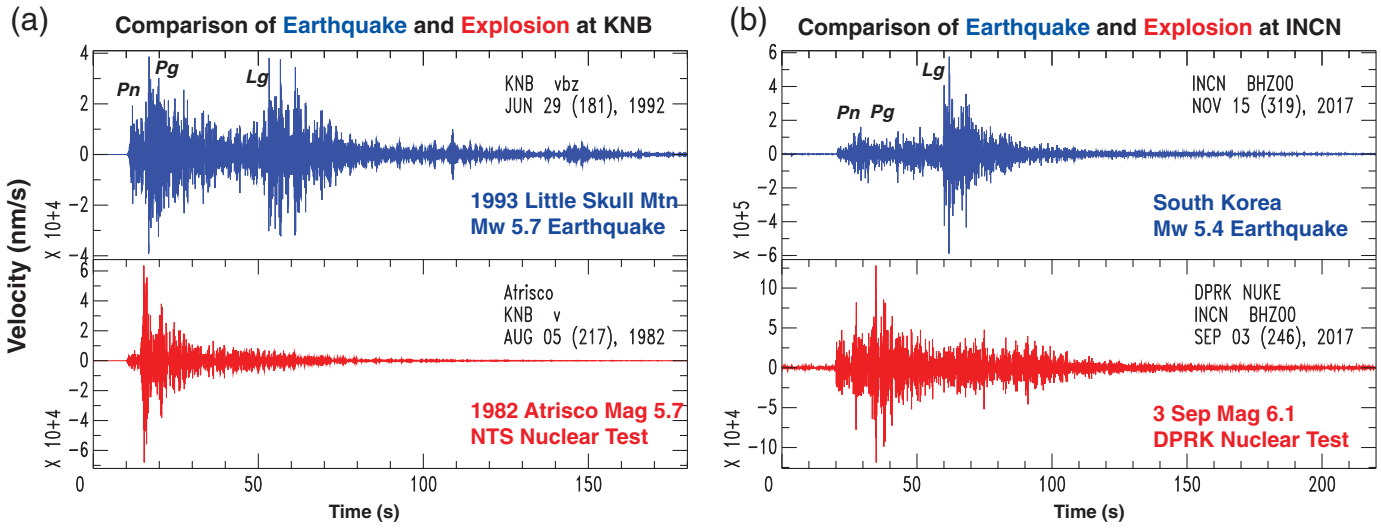

▲ **Figure 1.** Earthquake (blue) and explosion (red) 4–8 Hz band-pass filtered seismograms observed at a common station. (a) The Atrisco nuclear explosion and Little Skull Mountain earthquake at station KNB about 300 km away. (b) The 15 November 2017 South Korean earthquake and the 3 September 2017 Democratic People's Republic of Korea (DPRK) declared nuclear test at station INCN. The explosion is about 475 km away and the earthquake is about 285 km away. In each case, the relative absence of *Lg* amplitude for the explosions is a basis for identifying them.

period waveform modeling that can be challenging for events smaller than roughly magnitude 3.5 due to poor signal-to-noise values at these periods. We explore body-wave-based methods such as ratios of regional phase amplitudes, which may be applicable to event identification at much smaller magnitudes. We examine *P*/*S* amplitude ratios, such as a (2–4 Hz *Pn*)/(2–4 Hz *Lg*), and low/high-frequency spectral amplitude ratios within the same phase, such as a (2–4 Hz *Lg*)/(4–6 Hz *Lg*) (e.g., Walter *et al.*, 1995).

ANALYSIS

Explosion Versus Earthquake

The classic difference between earthquake and explosion *P*/*S* amplitudes observed in regional high-frequency seismic waveforms is illustrated in Figure 1. We show that for earthquake–explosion pairs observed in Nevada, U.S.A., and on the Korean Peninsula, the explosions are relatively deficient in *S*-wave energy. The seismograms in Figure 1 were all band-pass filtered between 4 and 8 Hz. The 1982 United States underground nuclear test named Atrisco, with an announced yield of 138 kt (U.S. Department of Energy [U.S. DOE], 2015) and a magnitude of 5.7, is compared with the nearby 1993 magnitude 5.7 Little Skull Mountain earthquake at station KNB about 300 km to the east in Utah. Note the strong amplitude *Lg* phase observed in the earthquake seismogram and its complete absence in the explosion seismogram. Similarly, the 15 November 2017 magnitude 5.4 earthquake in South Korea shows a very strong *Lg* amplitude at station INCN about 280 km to the west, while the 3 September 2017 DPRK declared nuclear test shows almost no distinct *S*-wave amplitude at the same station. This difference in relative *P*/*S* amplitudes, observed at regional distances and at frequencies > ~2 Hz, is the basis for an earthquake–explosion discriminant.

When comparing the regional phase amplitudes of events spread across a geographic region, some care must be taken to account for propagation effects, which can also change *P*/*S* ratios (e.g., Taylor and Hartse, 1998; Taylor *et al.*, 2002; Pasyanos and Walter, 2009). Here, we use 1D geometrical spreading and attenuation corrections appropriate to each region following the magnitude and distance amplitude correction (MDAC) procedure of Walter and Taylor (2001). The path-corrected 2–4 Hz *Pn*/*Lg* and *Pg*/*Lg* values averaged over the three components at station MDJ in northeast China are shown in Figure 2. They are plotted versus moment magnitude estimated for the six DPRK declared tests, and a variety of presumed crustal earthquakes in the Korean Peninsula, Yellow Sea, and northeast China (for a map of earthquakes, see Walter *et al.*, 2007). Because of the large difference in crustal thickness and the potential for *Lg* blocking (e.g., McNamara and Walter, 2001), we do not include events that have paths crossing the oceanic crust in the Sea of Japan. Figure 2 shows good separation between the explosions and earthquakes, similar to what has previously been observed for the earlier tests (e.g., Richards and Kim, 2007; Walter *et al.*, 2007; Zhao *et al.*, 2008, 2017; Shin *et al.*, 2010; Kim *et al.*, 2017).

The 2–4 Hz *Pn*/*Lg* values are independent of magnitude as expected (e.g., Walter *et al.*, 1995), whereas the 2–4 Hz *Pg*/*Lg* explosions show an apparent magnitude dependence. Curiously, the magnitude dependence is only observed on the horizontal components and not the vertical ones. In Figure 2, we show the MDJ east component for the six tests and it is clear that the *Pg* amplitude increases relative to the *Pn* and *Lg* phases as the magnitude increases. We suspect this may actually be a topographic scattering and/or depth effect, since the 2006

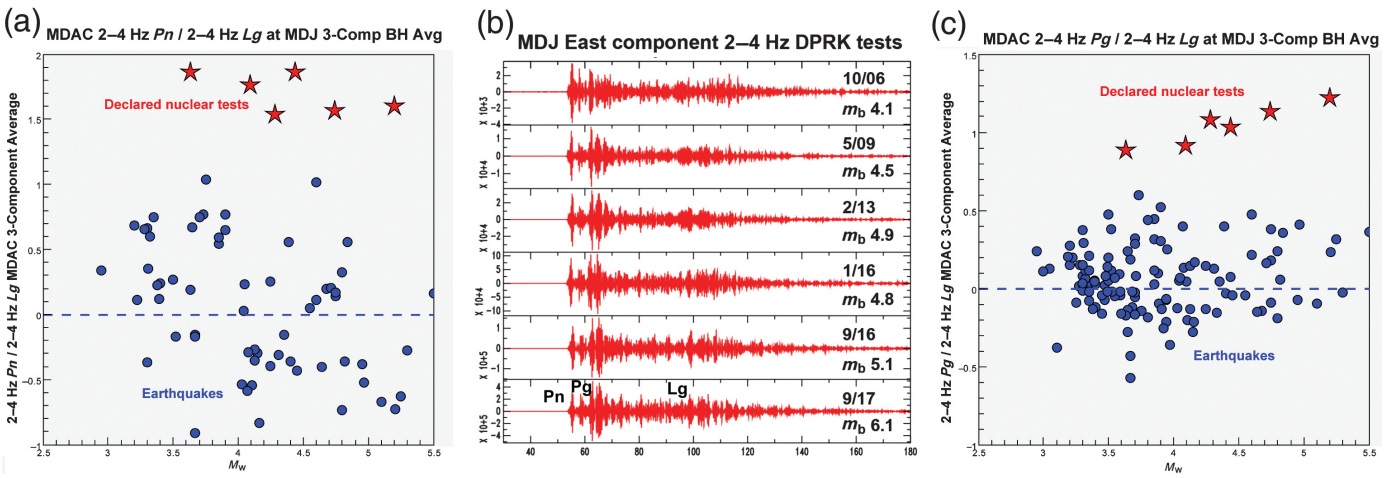

▲ **Figure 2.** *P*/*S* ratios and seismograms at MDJ. (a) MDAC 2–4 Hz three-component averaged *Pn*/*Lg* at MDJ versus magnitude. (b) 2–4 Hz band-pass filtered seismograms on the east component of MDJ for the six DPRK declared nuclear tests. (c) 2–4 Hz three-component averaged *Pg*/*Lg* at MDJ versus magnitude.

test is located a few kilometers east of the others and the inferred depth of the last three DPRK tests is greater than the earlier ones (e.g., Myers *et al.*, 2018; Pasyanos and Myers, 2018). Investigating regional phase behavior, such as *Pg* and *Lg* excitation as a function of depth and topography, is a good subject for future research, but beyond the scope of this article.

Postexplosion Collapse

The event that occurs eight and a half minutes after the 3 September 2017 declared nuclear test is well fit as a collapse mechanism using intermediate-period regional waveform modeling methods (e.g., Chiang *et al.*, 2018; Liu *et al.*, 2018). The size of this event is also roughly consistent with a gravitational collapse of a cavity roughly the size of that estimated to be formed by the nuclear test. We note that collapses of the vaporization cavity formed by a nuclear test in the minutes to hours to days following the explosion was not uncommon at the Nevada test site (NTS) (e.g., Springer *et al.*, 2002). For example, the 1982 m_b 5.7, M_s 4.2 Atrisco nuclear test was followed about 20 min later by a collapse seismic event with a magnitude of m_b 4.0 and M_s 3.5. It resulted in a crater about 359 m in diameter and 34 m deep (Springer *et al.*, 2002). However, not all nuclear tests that show seismic signs of collapse form surface craters. The issue of the stability of the vaporization cavity following a test depends upon many factors including geology and depth. In the case of the 3 September DPRK declared nuclear test, there are signs of surface subsidence (e.g., Pabian and Coblentz, 2018), but not a classic crater.

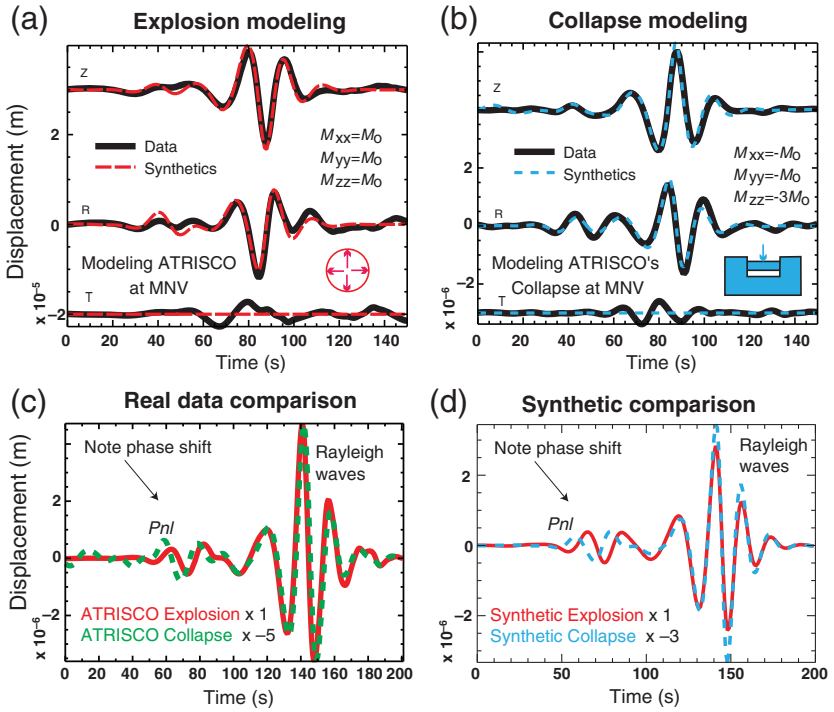

▲ **Figure 3.** Comparison of the Atrisco explosion and collapse waveforms at station MNV. (a) Data compared to pure explosion synthetics filtered between 15 and 50 s period. (b) Data compared to pure gravitational collapse synthetics filtered between 15 and 50 s period. (c) Comparison of explosion and scaled collapse data. (d) The same comparison for the synthetics.

In the case of Atrisco, the intermediate period waves from the explosion and the collapse are compared with model seismograms and each other in Figure 3. The figure shows the collapse Rayleigh waves have the opposite polarity from those produced by the explosion. When fit by synthetic seismograms, the explosion to first order is consistent with an isotropic

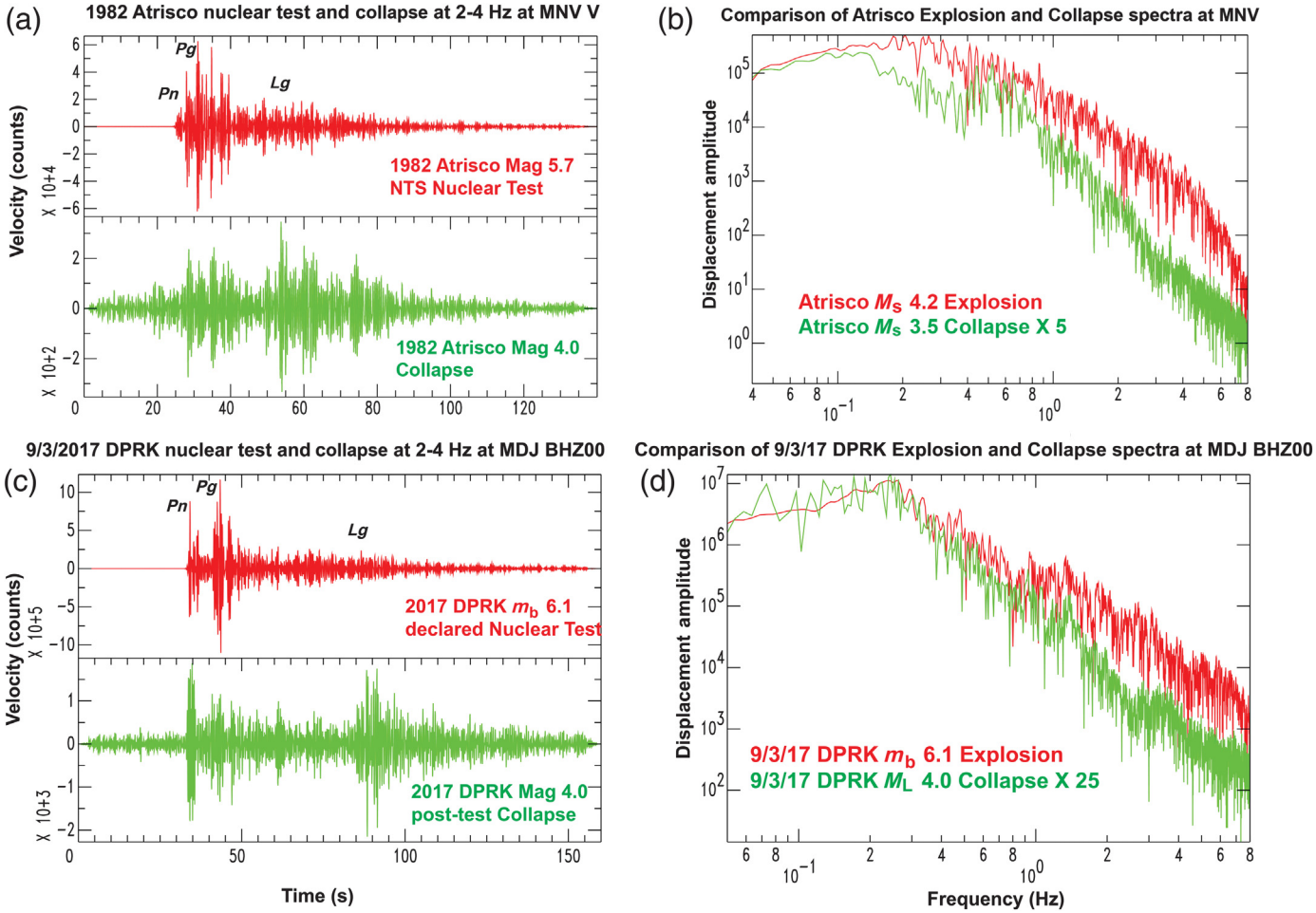

▲ **Figure 4.** Comparison of explosion and collapse seismograms and spectra. These are whole waveform spectral amplitudes and the collapses were multiplied by the scale factor to facilitate comparison. Note the collapses are relatively deficient in high-frequency energy compared with the explosions. (a) The Nevada test site (NTS) nuclear explosion Atrisco compared with its post-test collapse seismograms at station MNV. (b) Displacement spectra of Atrisco explosion and collapse at MNV, with the collapse spectral amplitudes are multiplied by a factor of 5. (c) The 3 September 2017 DPRK declared nuclear test compared with its inferred post-test collapse at station MDJ. (d) Displacement spectra of the DPRK explosion and collapse where the collapse spectral amplitudes are multiplied by 25.

source, and the collapse is well fit by a closing crack. By scaling the collapse by a factor of −5, and comparing the waveforms to each other, we see the Rayleigh waves nearly overlie, but the *Pnl* waves are different, consistent with a model where the collapse has a greater relative component of vertical dipole or M_{zz} component energy than the explosion (Walter, 1995). This is consistent with the Atrisco collapse model as a tabular failure under gravity rather than an implosion or the inverse of the nuclear explosion.

Another notable feature of postexplosion collapse waveforms is their relative lack of high-frequency energy when compared with the explosion waveforms. In Figure 4a, we compare the Atrisco explosion and it's subsequent collapse waveforms and full seismogram spectra to each other at regional station MNV. The collapse has a steeper spectral fall-off between 1 and 8 Hz and overall less relative high-frequency energy as compared with the explosion. In Figure 4b, we compare the 3 September 2017 DPRK declared nuclear explosion spectra with the subsequent collapse seismograms and full waveform spectra at MDJ. Again, the collapse has a steeper fall-off between 1 and 8 Hz and less high-frequency energy relative to the explosion.

One way to quantify the difference in relative high-frequency energy content is through ratios of low- to high-frequency energy. When the ratios are done on the same phase they are known as spectral ratios and when done between two different phases, such as low-frequency *P* to high-frequency *Lg*, they are known as cross-spectral ratios (e.g., Hartse *et al.*, 1997). We show in Figure 5 that for spectral ratios of low-frequency *S* waves to high-frequency *S* waves, the collapse has a much higher value than the earthquakes and the nuclear tests. For the DPRK region, these spectral ratios appear to be able to discriminate and identify the shallow collapse event from nuclear tests and earthquakes.

In other regions with weaker near-surface material, such as the former NTS, we have found that spectral ratios can sometimes separate nuclear tests from earthquakes. In particular, nuclear tests conducted in high gas-filled porosity material such

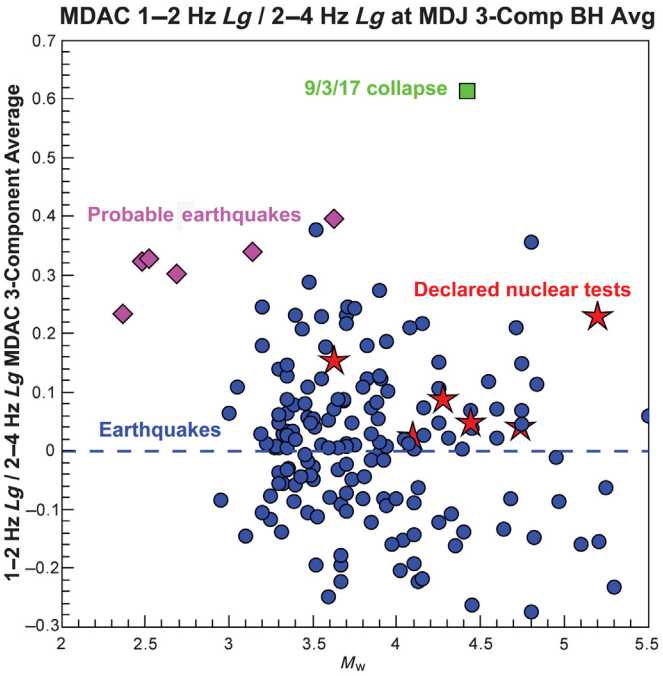

▲ **Figure 5.** Spectral ratio at MDJ can discriminate the collapse event. MDAC 1–2 Hz *Lg*/2–4 Hz *Lg* three-component averaged values versus magnitude from station MDJ are shown. Note the post-explosion collapse (green square) has high values and separates from the explosions (red stars) and the tectonic earthquakes (blue circles) and probable earthquakes (magenta diamonds).

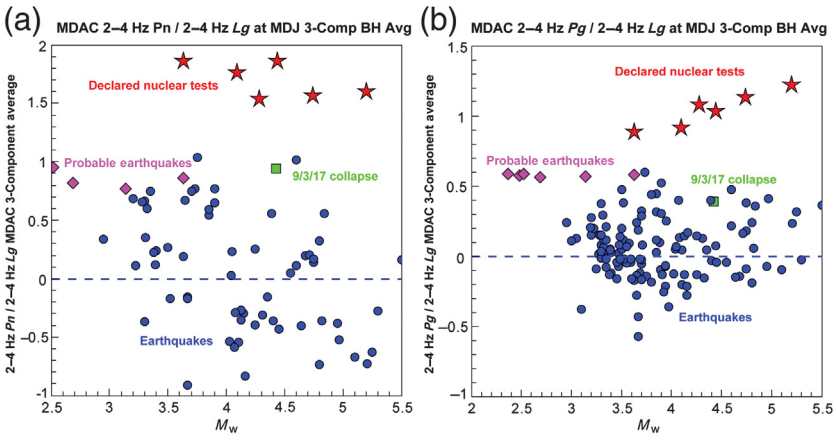

▲ **Figure 6.** *P*/*S* ratios at MDJ. (a) MDAC 2–4 Hz *Pn*/*Lg* three-component averaged values at MDJ are plotted versus magnitude are shown. (b) MDAC 2–4 Hz *Pg*/*Lg* three-component averaged values at MDJ versus magnitude are shown. Note the postexplosion collapse (green square) and the probable earthquakes (magenta diamonds) plot with the tectonic earthquakes (blue circles) in the region, whereas the explosions (red stars) clearly have higher values and separate from the other events.

as dry alluvium and tuff discriminate from earthquakes using low- to high-frequency *Lg* spectral ratios (Walter *et al.*, 1995). As Figure 2 shows, that is not the case for the DPRK region. Interestingly, if we form *P*/*S* ratios in the same frequency band, such as at 2–4 Hz as shown in Figure 6, the collapse event then plots with the earthquakes and separates from the explosions. By combining *P*/*S* and low- to high-frequency ratios, it appears that we may be able to uniquely identify the collapse events in both soft- and hard-rock geologies.

Probable Earthquakes

An uncommon feature of the 3 September 2017 DPRK declared nuclear explosion is the detection and location of nearby seismic events following the test by the USGS and the IDC. These included an m_b 2.6 event at 04:43 on 23 September 2017 (IDC), an m_b 3.4 event at 08:29 also on 23 September 2017 (IDC), and an event on 16:41 on 12 October 2017 (USGS). In Figure 7, we show seismograms of these events at MDJ as well as their spectra. We note that based on the *P*/*S* values shown in Figure 6, they plot with the earthquake population and are not deficient in high frequency like the collapse event. We note that these events do not form clusters that have time of day or other characteristics associated with mine blasts. For these reasons, we will refer to these events as probable earthquakes.

We used these probable earthquakes as templates in a waveform correlation search and discovered there are a number of other related events, some of which occurred before the 2017 test. Details of this analysis are reported by Dodge (2018) and similar findings are reported by Gibbons *et al.* (2018). We note that related events occurred in 2014 and perhaps as early as 2011. As discussed by Dodge (2018), these events do not follow the normal Omori law decay curves of an aftershock sequence in relation to any of the DPRK declared nuclear explosions. Myers *et al.* (2018) locate these events 4–8 km north of the DPRK test site. For these reasons, we do not believe they should be referred to as "aftershocks" of the 3 September 2017 declared nuclear explosion. It is possible these events are related and perhaps even induced by the explosion activity at the DPRK test site. It is also possible that in this moderately active seismic region they are simply natural tectonic earthquakes. Body-wave analysis does not show any special features of these probable earthquakes as compared to the background tectonic earthquakes. Any special relationship between these probable earthquakes, the other events that correlate with them (except of course the collapse), and the DPRK declared nuclear explosions will need to depend on inferences from timing and location information or from more local seismic data.

We used the correlation results of Dodge (2018) and looked at all events with an estimated magnitude greater than 2.5 at station MDJ. We found three additional events in December for which we were able to get good regional phase amplitude measurements between 1 and 4 Hz at station MDJ: 1 December 2017 at 22:45, 5 December 2017 at 14:40, and 9 December 2017 at 06:13. In Figure 6, we show the 2–4 Hz

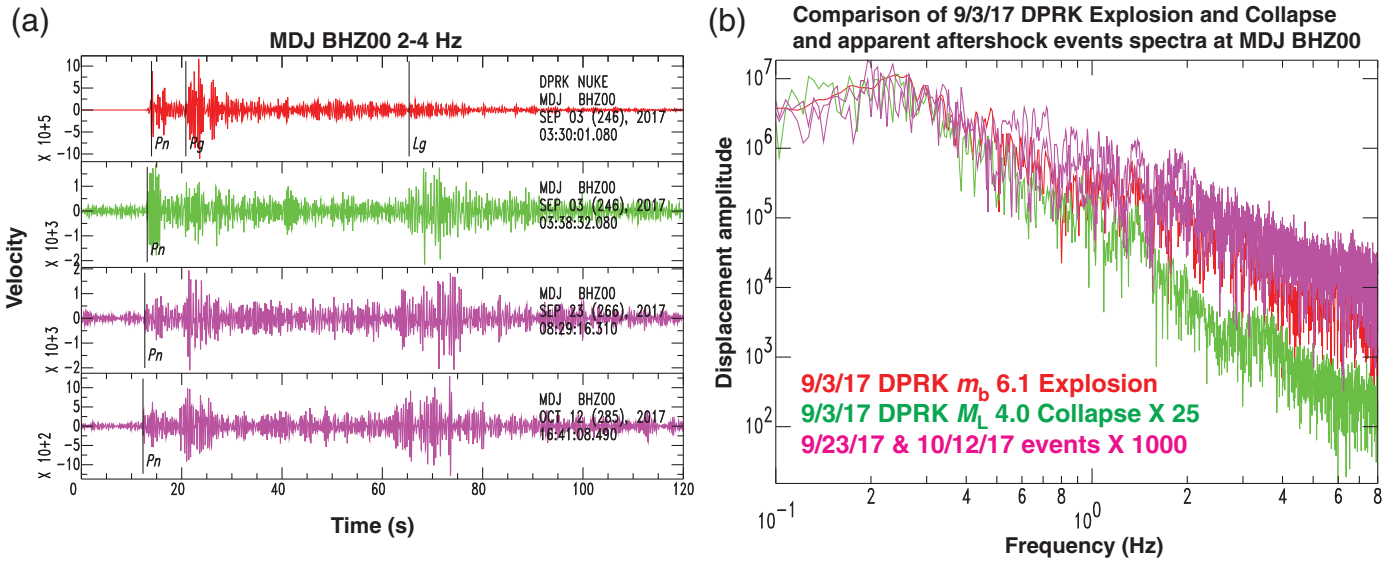

▲ **Figure 7.** Explosion, collapse, and inferred earthquakes. (a) Seismograms and (b) full waveform spectra. Note the probable earthquakes (pink) show clear *Lg* phases and are not deficient in high-frequency energy like the collapse (green).

Pn/*Lg* and *Pg*/*Lg* values of these probable earthquakes. We note they have very similar values to the natural tectonic earthquakes and the September and October 2017 probable earthquakes and clearly separate from the nuclear tests.

DISCUSSION

The ability to use seismic waves to discriminate between earthquakes, explosions, and collapses is an important component of nuclear explosion monitoring. Traditional techniques such as M_s–m_b have had problems in discriminating the DPRK explosions from earthquakes (e.g., Selby *et al.*, 2012). In contrast, newer techniques utilizing intermediate-period regional waveform modeling to determine moment tensors are very effective (e.g., Ford *et al.*, 2009, 2012; Chiang *et al.*, 2018). However, M_s–m_b and moment tensor techniques can be challenging to employ when the events become too small to easily see at periods below about 10 s, at roughly magnitudes < 3.5. These techniques can also be challenging to use when the source-to-station paths traverse complex Earth structure that is not well modeled by a 1D approximation. In such cases, 3D model synthetics might prove effective, but would require the development of appropriate Earth models.

Body-wave methods such as regional high-frequency *P*/*S* values have proven very effective since their widespread application in the mid 1990s. However, there remain concerns due to our incomplete understanding of how explosions generate *S* waves and the lack of a predictable explosion *S*-wave model. One way this issue is being addressed is through the Source Physics Experiments (SPE), a series of very densely instrumented chemical explosions in Nevada (Snelson *et al.*, 2013). Preliminary results from the SPE show that high-frequency *S* waves in hard rock are generated by driven motion on preexisting joints (e.g., Vorobiev *et al.*, 2018), whereas for lower frequency *S* waves the dominant mechanism appears to be the scattering and conversion of *P* and *Rg* waves due to heterogeneities around the source (e.g., Pitarka *et al.*, 2015). The scattering efficiency in terms of generating shear waves may be frequency dependent, which would help explain why *P*/*S* ratios at frequencies greater than 2 Hz are much more effective at earthquake–explosion discrimination than *P*/*S* ratios at frequencies below 2 Hz.

There are isolated instances where *P*/*S* values do not identify explosions very well, such as deeply buried (overburied from a scaled depth perspective) nuclear tests in the former Soviet Union (e.g., Pasyanos *et al.*, 2012). As we show in this article, *P*/*S* is quite effective as an earthquake–explosion discriminant for the six DPRK declared nuclear tests, despite the fact that some are likely quite overburied compared to practices at the NTS (e.g., Pasyanos and Myers, 2018). These DPRK results are encouraging for the use of *P*/*S* values for explosion identification down to very small sizes and significant overburial, but more work is needed via experiments such as the SPE and numerical modeling to reconcile the outlier behavior of some overburied events.

Finally, in this article we show that combination of *P*/*S* values and spectral ratios in the *S* waves between low and higher frequency bands can identify collapse events and separate them from both explosions and earthquakes. These results are also encouraging for finding postexplosion collapse events in cases where moment tensor methods may not be applicable due to signal-to-noise conditions or other waveform modeling complications.

CONCLUSIONS

In this article, we have shown that regional body-wave phases (e.g., *Pn*, *Pg*, *Sn*, *Lg*) can be used to separate the populations of different seismic source types down to very low magnitudes. We show that *P*/*S* values at frequencies of about 2 Hz and

higher can discriminate the six DPRK declared nuclear tests from a background of tectonic earthquakes. We show that low- to high-frequency ratios, alone or when combined with P/S values, can discriminate the 3 September 2017 post-test apparent collapse from both the explosions and the tectonic earthquakes. Finally, we look at the seismic events on 23 September, 12 October 2017, 1, 5, and 9 December 2017, and find they have P/S and low- to high-frequency values consistent with tectonic earthquakes. Given these body-wave signatures and that these events appear to be located kilometers north of the test site, we infer they appear to be earthquakes, very similar in nature to other tectonic earthquakes in the region.

DATA AND RESOURCES

The facilities of Incorporated Research Institutions for Seismology (IRIS) Data Services, and specifically the IRIS Data Management Center, were used for access to waveforms used in this study. IRIS Data Services are funded through the Seismological Facilities for the Advancement of Geoscience and EarthScope (SAGE) Proposal of the National Science Foundation under Cooperative Agreement EAR-1261681.

ACKNOWLEDGMENTS

The authors thank Stan Ruppert and Terri Hauk for their long-term work to build and maintain the Lawrence Livermore National Laboratory (LLNL) research database. The authors thank Editor-in-Chief Zhigang Peng, and two anonymous reviewers for comments that improved the article. This work was performed in part under the auspices of the U.S. Department of Energy by LLNL under Contract Number DE-AC52-07NA27344. Lawrence Livermore National Security, LLC. This is LLNL Contribution Number LLNL-JRNL-750362.

REFERENCES

Battone, S., M. D. Fisk, and G. D. McCarter (2002). Regional seismic-event characterization using a Bayesian formulation of simple kriging, *Bull. Seismol. Soc. Am.* **92,** 2277–2296.

Bowers, D., and N. D. Selby (2009). Forensic seismology and the comprehensive nuclear-test-ban treaty, *Annu. Rev. Earth Planet. Sci.* **37,** 209–236, doi: 10.1146/annurev.earth.36.031207.124143.

Bowers, D., and W. R. Walter (2002). Discriminating between large mine collapses and explosions using teleseismic *P*-waves, *Pure Appl. Geophys.* **159,** 803–830.

Chiang, A., D. S. Dreger, S. R. Ford, G. Ichinose, E. Matzel, W. R. Walter, and S. Myers (2018). Moment tensor source-type analysis for the Democratic People's Republic of Korea declared nuclear explosions (2006–2017) and 03 Sep 2017 collapse event, *Seismol. Res. Lett.* doi: 10.1785/0220180130.

Dodge, D. (2018). Searching for induced seismicity at Punggye-ri nuclear test site using subspace detectors, *Seismol. Res. Lett.* doi: 10.1785/0220180127.

Ford, S. R., D. S. Dreger, and W. R. Walter (2009). Source analysis of the memorial day explosion, Kimchaek, North Korea, *Geophys. Res. Lett.* **36,** L21304, doi: 10.1029/2009GL040003.

Ford, S. R., W. R. Walter, and D. S. Dreger (2012). Event discrimination using regional moment tensors with teleseismic *P* constraints, *Bull. Seismol. Soc. Am.* **102,** no. 2, 867–872, doi: 10.1785/0120110227.

Gibbons, S. J., T. Kvaerna, S. P. Nasholm, and S. Mykkeltveit (2018). Probing the DPRK nuclear test site down to low-seismic magnitude, *Seismol. Res. Lett.* doi: 10.1785/0220180116.

Hartse, H., S. R. Taylor, W. S. Phillips, and G. E. Randall (1997). A preliminary study of regional seismic discrimination in Central Asia with an emphasis on Western China, *Bull. Seismol. Soc. Am.* **87,** 551–568.

Kim, W.-Y., V. Aharonian, A. L. Lerner-Lam, and P. G. Richards (1997). Discrimination of earthquakes and explosions in Southern Russia using regional high frequency three-component data from the IRIS/JSP Caucasus network, *Bull. Seismol. Soc. Am.* **87,** 569–588.

Kim, W.-Y., P. G. Richards, D. P. Schaff, and K. Koch (2017). Evaluation of a seismic event, 12 May 2010, in North Korea, *Bull. Seismol. Soc. Am.* **107,** 1–21, doi: 10.1785/0120160111.

Liu, J., L. Li, J. Zahradnik, E. Sokos, C. Liu, and X. Tian (2018). North Korea's 2017 test and its non-tectonic aftershock, *Geophys. Res. Lett.* **45,** no. 7, 3017–3025, doi: 10.1002/2018GL077095.

McNamara, D. E., and W. R. Walter (2001). Mapping crustal heterogeneity using Lg propagation efficiency throughout the Middle East, Mediterranean, Southern Europe and North Africa, *Pure Appl. Geophys.* **158,** 1165–1188.

Mine Seismicity and the Comprehensive Nuclear-Test-Ban Treaty (1999). Report of a Working group: F. Chiappetta, F. Heuze (co-chair), R. Hoppler, V. Hsu, B. Martin, C. Pearson, B. Stump (co-chair), W. Walter, and K. Zipf. Released draft in March 1997, review by National Academy of Sciences Panel issued July 1998, revised and released in final form as DOE report in April 1999, *LLNL Report UCRL-ID-132897*, 70 pp.

Myers, S. C., S. R. Ford, R. J. Mellors, and G. Ichinose (2018). Absolute locations of the North Korean nuclear tests based on differential seismic arrival times and InSAR, *Seismol. Res. Lett.* doi: 10.1785/0220180123.

National Research Council (NRC) (2012). *The Comprehensive Nuclear Test Ban Treaty: Technical Issues for the United States*, The National Academies Press, Washington, D.C., 204 pp.; available at https://www.nap.edu/catalog/12849/the-comprehensive-nuclear-test-ban-treaty-technical-issues-for-the (last accessed September 2018).

Pabian, F., and D. Coblentz (2018). Observed surface disturbances associated with the DPRK's 3 September 2017 underground nuclear test, *Seismol. Res. Lett.* doi: 10.1785/0220180120.

Pasyanos, M. E., and S. C. Myers (2018). The coupled location/depth/yield problem for North Koreas declared nuclear tests, *Seismol. Res. Lett.* doi: 10.1785/0220180109.

Pasyanos, M. E., and W. R. Walter (2009). Improvements to regional explosion identification using attenuation models of the lithosphere, *Geophys. Res. Lett.* **36,** L14304, doi: 10.1029/2009GL038505.

Pasyanos, M. E., S. R. Ford, and W. R. Walter (2012). Testing event discrimination over broad regions using the historical Borovoye observatory explosion dataset, *Pure Appl. Geophys.* doi: 10.1007/s00024-012-0591-4 (published online 20 September 2012).

Pechmann, J. C., W. R. Walter, S. J. Nava, and W. J. Arabasz, (1995). The February 3, 1995 M_L 5.1 seismic event in the trona mining district of southwestern Wyoming, *Seismol. Res. Lett.* **66,** 25–34,

Pitarka, A., R. J. Mellors, W. R. Walter, S. Ezzedine, O. Vorobiev, T. Antoun, J. L. Wagoner, E. M. Matzel, S. R. Ford, A. J. Rodgers, *et al.* (2015). Analysis of ground motion from an underground chemical explosion, *Bull. Seismol. Soc. Am.* **105,** no. 5, 2390–2410, doi: 10.1785/0120150066.

Richards, P. G., and W. Y. Kim (2007). Seismic signature, *Nat. Phys.* **3,** no. 1, 4–6, doi: 10.1038/Nphys495.

Rodgers, A. J., and W. R. Walter (2002). Seismic discrimination of the May 11, 1998 Indian nuclear test with short-period regional data from station NIL (Nilore, Pakistan), *Pure Appl. Geophys.* **159,** no. 4, 679–700, doi: 10.1007/s00024-002-8654-6.

Selby, N. D., P. D. Marshall, and D. Bowers (2012). $m_b : M_s$ event screening revisited, *Bull. Seismol. Soc. Am.* **102,** 88–97.

Shin, J. S., D. H. Sheen, and G. Kim (2010). Regional observations of the second North Korean nuclear test on 2009 May 25, *Geophys. J. Int.* **180,** no. 1, 243–250, doi: 10.1111/j.1365-246X.2009.04422.x.

Snelson, C., R. Abbott, S. Broome, R. Mellors, H. Patton, A. Sussman, M. Townsend, and W. Walter (2013). Source Physics Experiment to validate a new paradigm for nuclear test monitoring, *EOS Trans. AGU* **94,** no. 27, 237–239.

Springer, D. L., G. A. Pawloski, J. L. Ricca, R. Roher, and D. K. Smith (2002). Seismic source summary for all U.S. below surface nuclear explosions, *Bull. Seismol. Soc. Am.* **92,** 1806–1840.

Taylor, S. R. (1994). False alarms and mine seismicity: An example from the Gentry Mountain mining region, Utah, *Bull. Seismol. Soc. Am.* **84,** 350–358.

Taylor, S. R. (1996). Analysis of high-frequency *Pg/Lg* ratios from NTS explosions and Western U.S. earthquakes, *Bull. Seismol. Soc. Am.* **86,** 1042–1053.

Taylor, S. R., and H. E. Hartse (1998). A procedure for estimation of source and propagation amplitude corrections for regional seismic discriminants, *J. Geophys. Res.* **103,** doi: 10.1029/97JB03292.

Taylor, S. R., A. A. Velasco, H. E. Hartse, W. S. Phillips, W. R. Walter, and A. J. Rodgers (2002). Amplitude corrections for regional seismic discriminants, *Pure Appl. Geophys.* **159,** 623–650.

U.S. Department of Energy (U.S. DOE) (2015). *United States Nuclear Tests July 1945-September 1992, DOE/NV-209-REV16*, available at https://www.nnss.gov/docs/docs_LibraryPublications/DOE_NV-209_Rev16.pdf (last accessed July 2018).

Vorobiev, O., R. Hurley, and S. Ezzedine (2018). Near-field non-radial motion generation from underground explosions in jointed granite, *Geophys. J. Int.* **212,** 25–41, doi: 10.1093/gji/ggx403.

Walter, W. R. (1995). Status report on new whole waveform discriminants and preliminary results (deliverable #12), *Lawrence Livermore National Laboratory Technical Rept. UCRL-ID-123227*, available at https://www.osti.gov/servlets/purl/231382 (last accessed September 2018).

Walter, W. R., and S. R. Taylor (2001). A revised magnitude and distance amplitude correction (MDAC2) procedure for regional seismic discriminants: Theory and testing at NTS, *Lawrence Livermore National Laboratory UCRL-ID-146882*, available at http://www.llnl.gov/tid/lof/documents/pdf/240563.pdf (last accessed September 2018).

Walter, W. R., E. Matzel, M. E. Pasyanos, D. B. Harris, R. Gok, and S. R. Ford (2007). Empirical observations of earthquake and explosion discrimination using P/S ratios and implications for the sources of explosion *S*-waves, *Proc. of the 29th annual Monitoring Research Review, LA-UR-07-5613, NNSA and AFRL*, Denver, Colorado, 25–27 September 2007, available at https://l2a.ucsd.edu/local/Meetings/2007_MRR/PAPERS/03-20.PDF (last accessed September 2018).

Walter, W. R., K. Mayeda, and H. J. Patton (1995). Phase and spectral ratio discrimination between NTS earthquakes and explosions Part 1: Empirical observations, *Bull. Seismol. Soc. Am.* **85,** 1050–1067.

Zhao, L.-F., X.-B. Xie, W.-M. Wang, N. Fan, X. Zhao, and Z.-X. Yao (2017). The 9 September 2016 North Korean underground nuclear test, *Bull. Seismol. Soc. Am.* **107,** no. 6, 3044–3051, doi: 10.1785/0120160355.

Zhao, L.-F., X.-B. Xie, W.-M. Wang, and Z.-X. Yao (2008). Regional seismic characteristics of the 9 October 2006 North Korean nuclear test, *Bull. Seismol. Soc. Am.* **98,** no. 6, 2571–2589, doi: 10.1785/0120080128.

William R. Walter
Douglas A. Dodge
Gene Ichinose
Stephen C. Myers
Michael E. Pasyanos
Sean R. Ford
Lawrence Livermore National Laboratory
L-046, 7000 East Avenue
Livermore, California 94550 U.S.A.
bwalter@llnl.gov

Published Online 26 September 2018